Electronic Supplementary Information (ESI)

Vapochromism Induced by Intermolecular Electron Transfer Coupled with Hydrogen-bond Formation in Zinc Dithiolene Complex

So Yokomori, Shun Dekura,* Tomoko Fujino, Mitsuaki Kawamura, Taisuke Ozaki, Hatsumi Mori*

The Institute for Solid State Physics, The University of Tokyo, Kashiwa, Chiba 2778581, Japan.

E-mail: s.dekura@issp.u-tokyo.ac.jp, hmori@issp.u-tokyo.ac.jp; Fax: +81 4 7136 3410; Tel: +81 4 7136 3410

Table of Contents

NMR spectra of compound 1, $(Ph_4P)_2[Zn(4\text{-mxbdt})_2]$

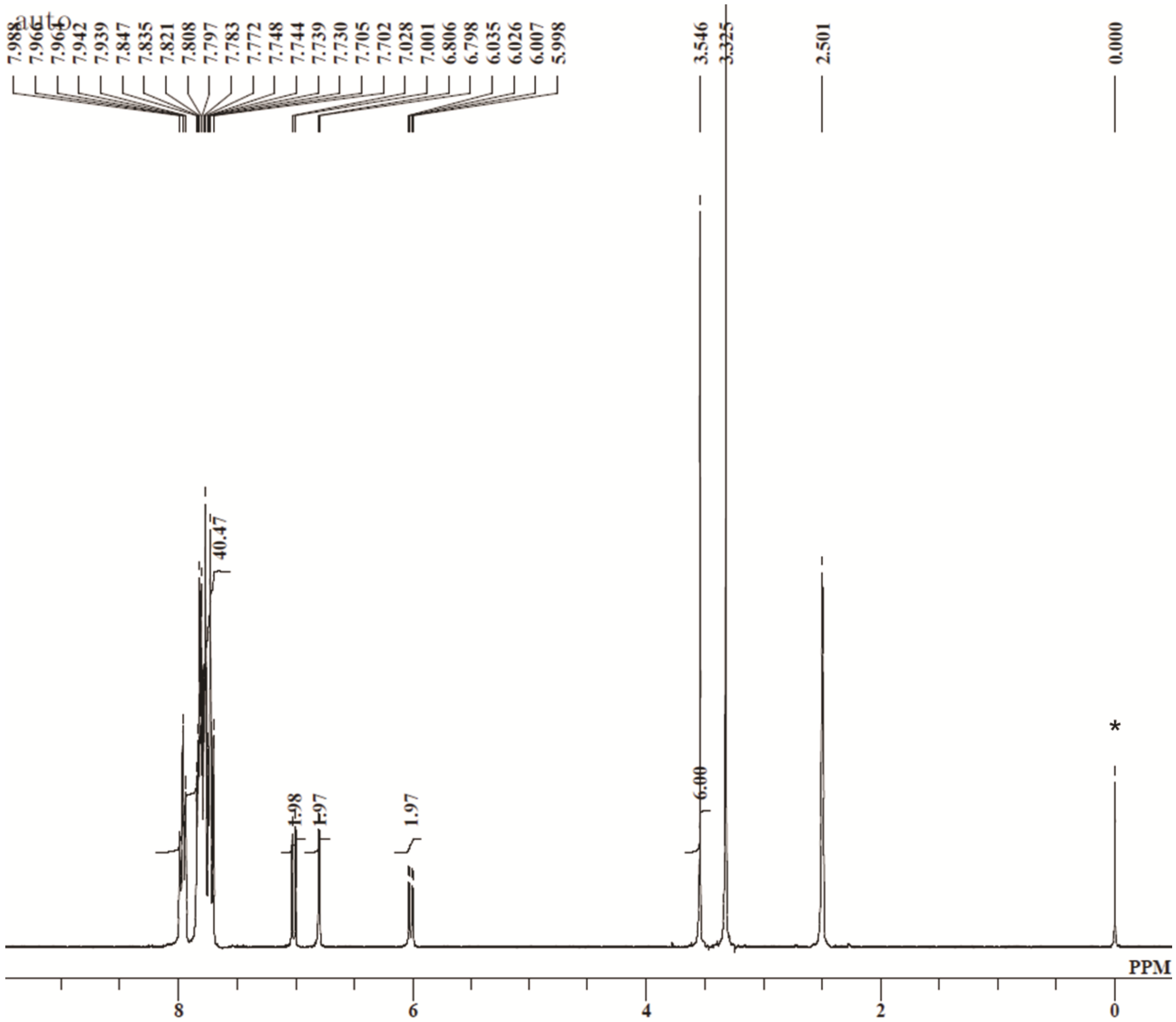

Fig. S1. ^{1}H NMR spectra of **1** (300 MHz, DMSO-d_6). An asterisk denotes a peak of Me_4Si as an internal standard.

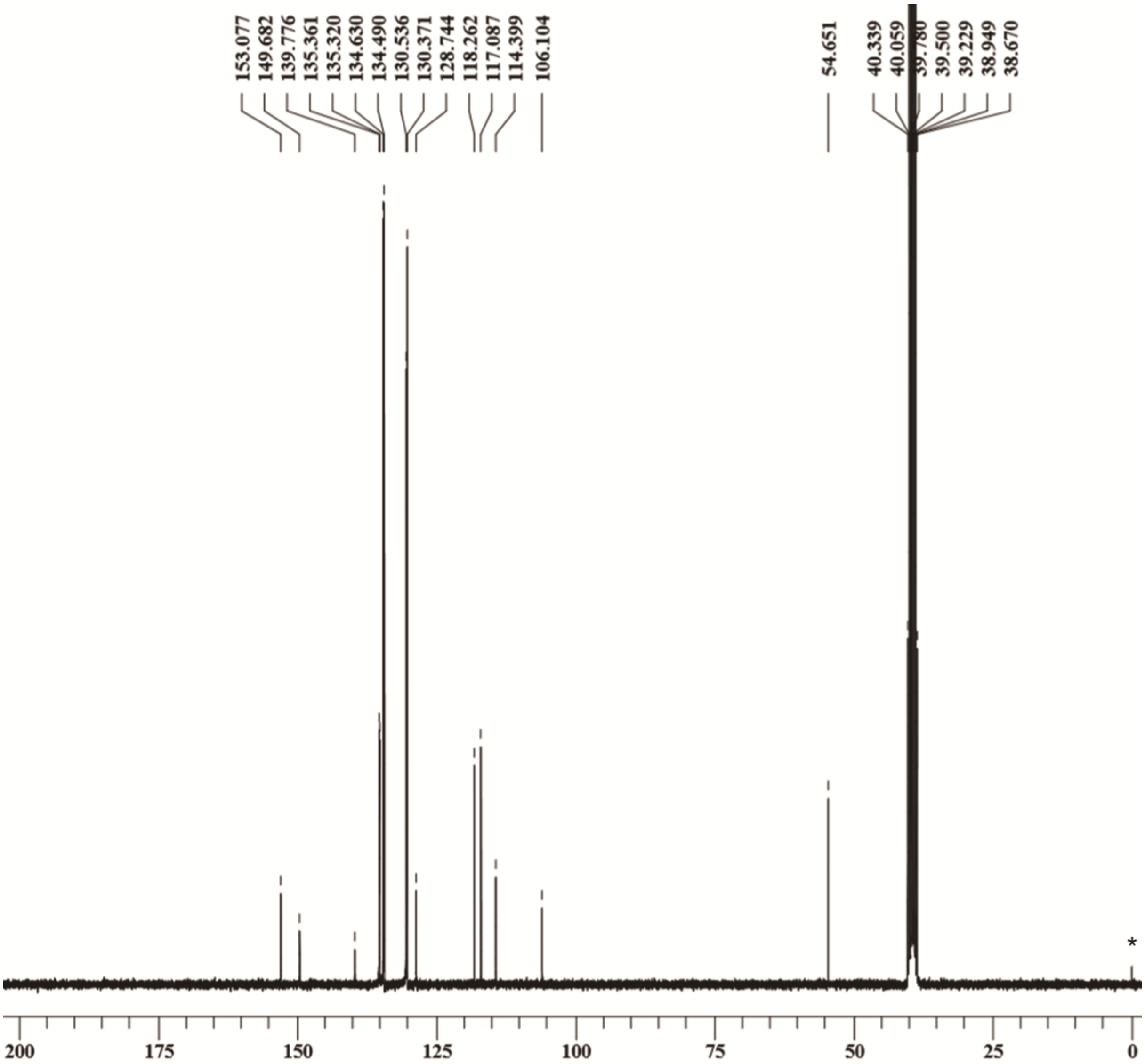

Fig. S2. ^{13}C NMR spectra of **1** (75 MHz, DMSO-d_6). An asterisk denotes a peak of Me_4Si as an internal standard.

Single-crystal X-ray diffraction (XRD) measurements

For **1**·2MeOH, because of the severely disordered MeOH molecules, the H atom in the O–H group of the disordered MeOH molecules did not reside on reasonable position in the refined structure. Therefore, we analyzed the crystal **1**·2MeOH without the H atoms on analysis.

Table S1. Crystallographic parameters for crystals **1**·2MeOH, **1**, and **1**·H_2O.

	1·2MeOH	**1**	**1**·H_2O
formula	$C_{64}H_{59}O_4P_2S_4Zn$	$C_{62}H_{52}O_2P_2S_4Zn$	$C_{62}H_{54}O_3P_2S_4Zn$
formula weight	1148.01	1084.66	1102.67
crystal system	monoclinic	monoclinic	monoclinic
space group	$P2_1/c$	$P2_1/c$	$P2_1/c$
a (Å)	22.5655(28)	22.2168(8)	22.7885(6)
b (Å)	12.3629(15)	11.6456(3)	11.5844(3)
c (Å)	22.0108(29)	21.9665(6)	22.2706(5)
α (deg.)	90	90	90
β (deg.)	111.7447(15)	110.865(4)	112.678(3)
γ (deg.)	90	90	90
V (Å^3)	5703.6(12)	5310.6(3)	5424.7(3)
Z	4	4	4
T (K)	200	200	200
D_{calc} (g·cm^{-3})	1.337	1.357	1.350
λ (Å)	0.71073	0.71073	0.71073
R_{int}	0.0462	0.0303	0.0263
R_1 (I>2.00σ(I))	0.0530	0.0791	0.0460
wR_2 (All reflections)	0.1512	0.2367	0.1376
GOF	1.092	1.173	1.126
CCDC	2016470	2016471	2016472

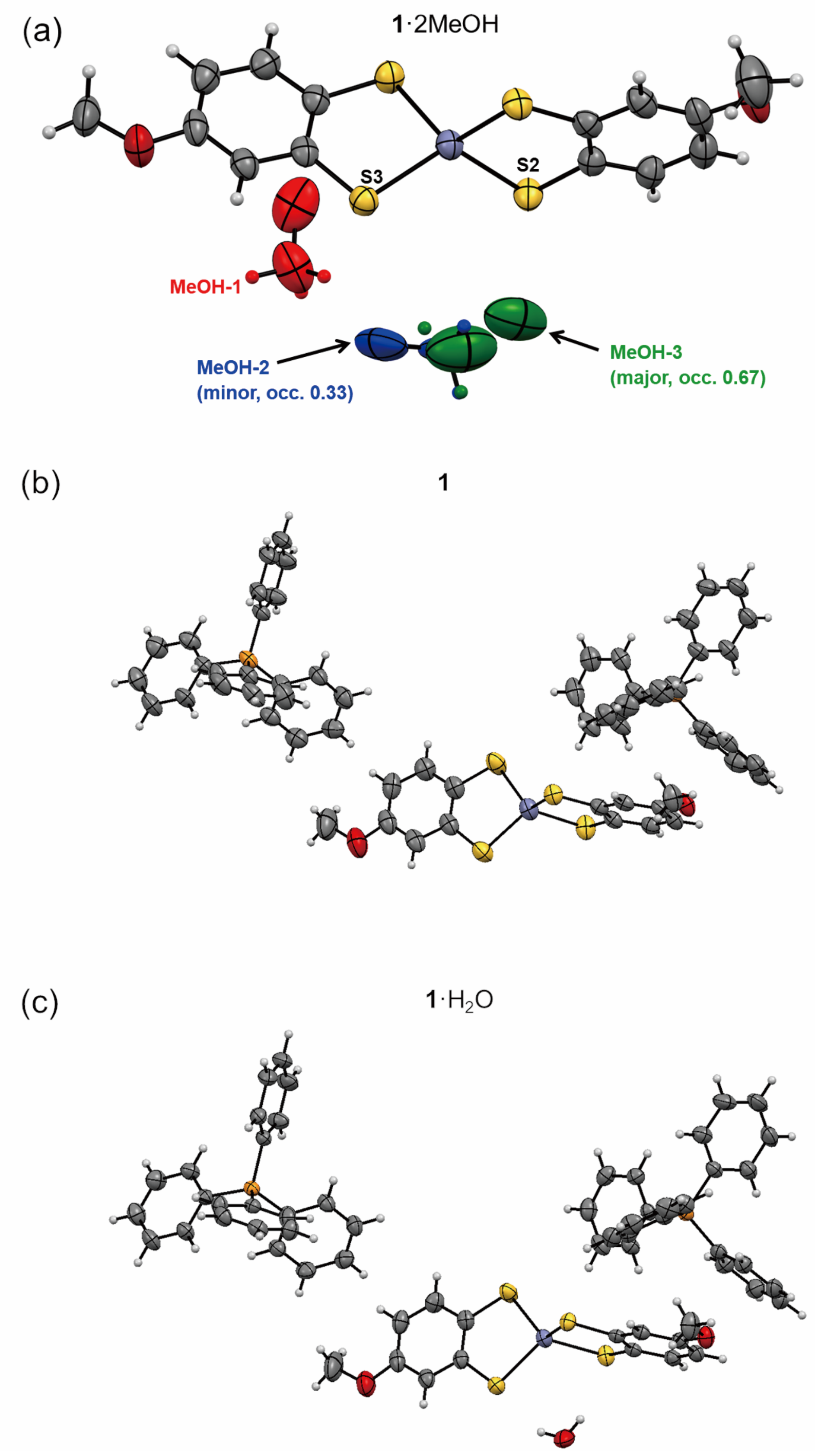

Fig. S3. (a) Positions of methanol molecules in **1**·2MeOH. (b), (c) The ORTEP drawing of crystal structures of (b) **1** and (c) **1**·H_2O (blue: Zn, yellow: S, orange: P, red: O, gray: C, white: H).

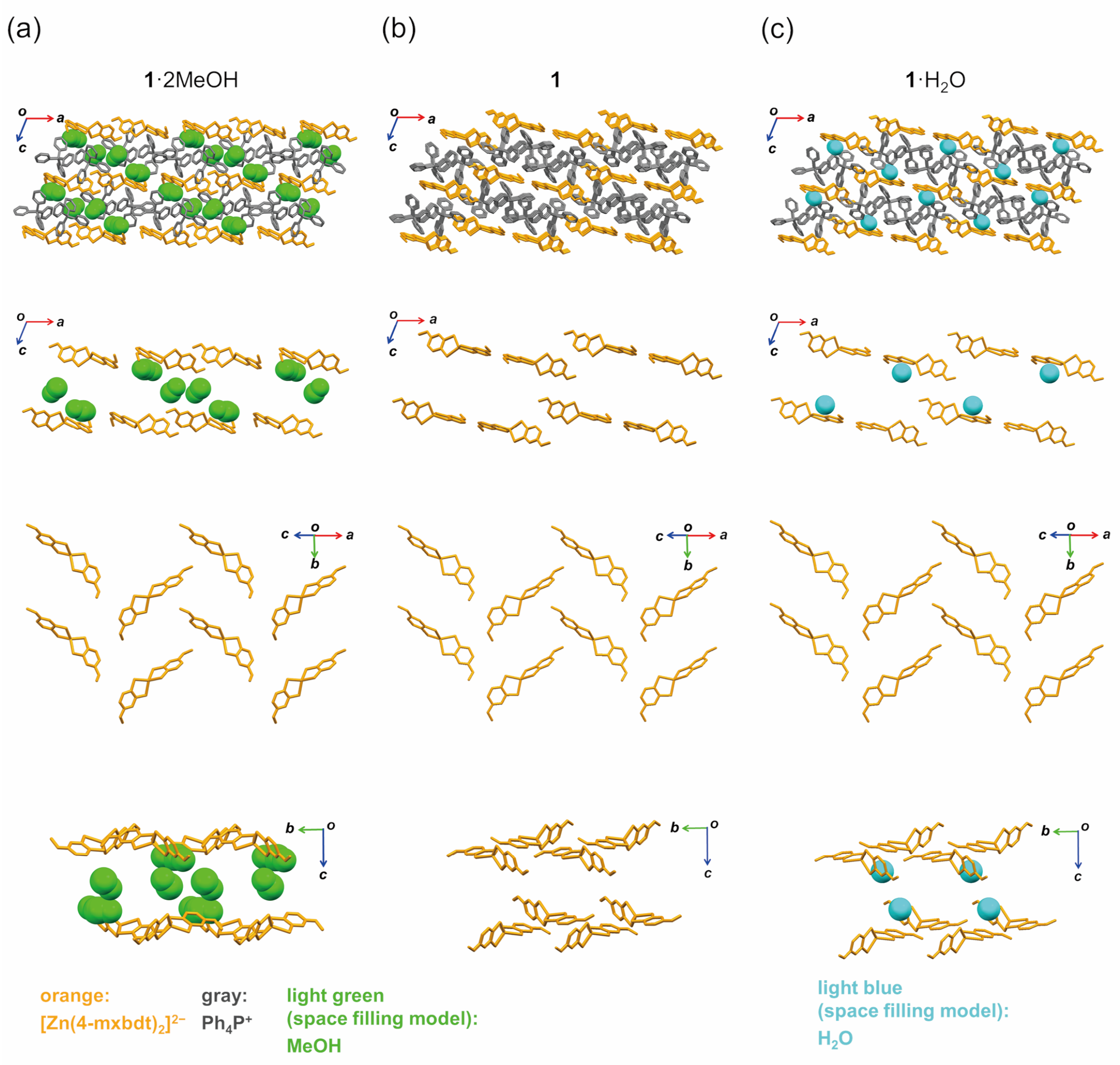

Fig. S4. Molecular arrangements of (a) **1**·2MeOH, (b) **1**, and (c) **1**·H_2O. The molecular arrangement of zinc complexes and Ph_4P^+ cations in **1**·H_2O hardly changed from those in **1**. Hydrogen atoms were omitted for clarity.

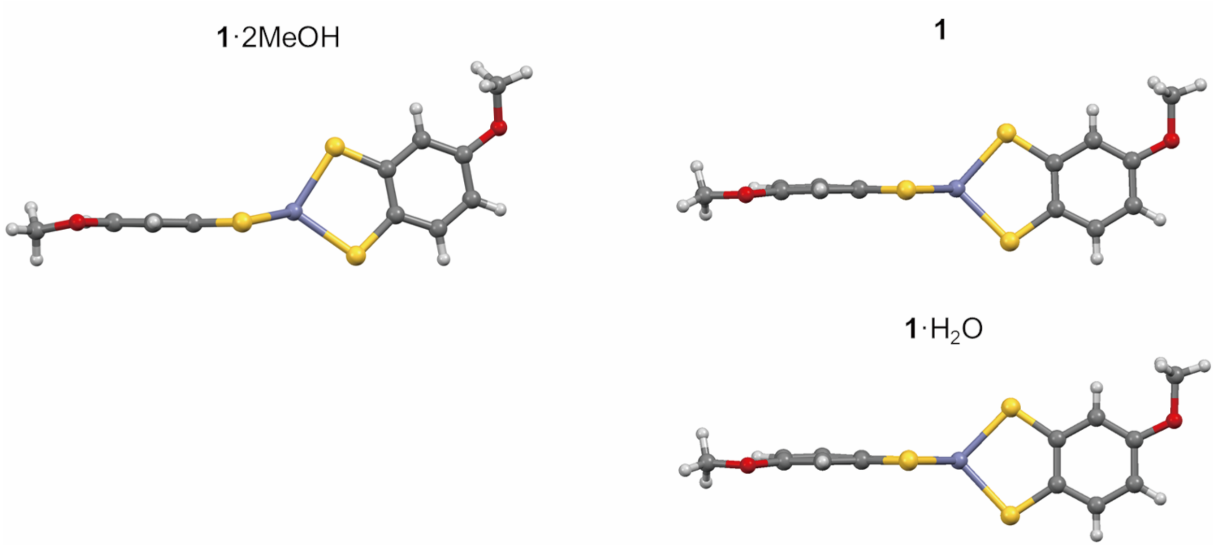
1·2MeOH

1

1·H_2O

Fig. S5. Molecular structures of $[Zn(4\text{-mxbdt})_2]^{2-}$ in **1**·2MeOH, **1**, and **1**·H_2O.

Powder X-ray diffraction patterns (PXRD)

As a result of PXRD measurements, sharp peaks were observed for both samples, which indicates their high crystallinity. The observed PXRD patterns (Fig. S6, red and blue solid line, respectively) were almost the same with the simulated patterns based on the structure determined by the single-crystal XRD measurements. Note that the peaks in the simulated patterns are slightly shifted to the high 2θ angles because the single-crystal XRD measurements were performed at 200 K whereas the PXRD measurements were performed at room temperature (Fig. S6). Here, the PXRD pattern of methanol adsorbed **1** included a few peaks originated from **1**. Considering the slight color change of the powder sample from yellow to orange during PXRD measurement, it is due to the partial desorption of methanol under atmospheric conditions.

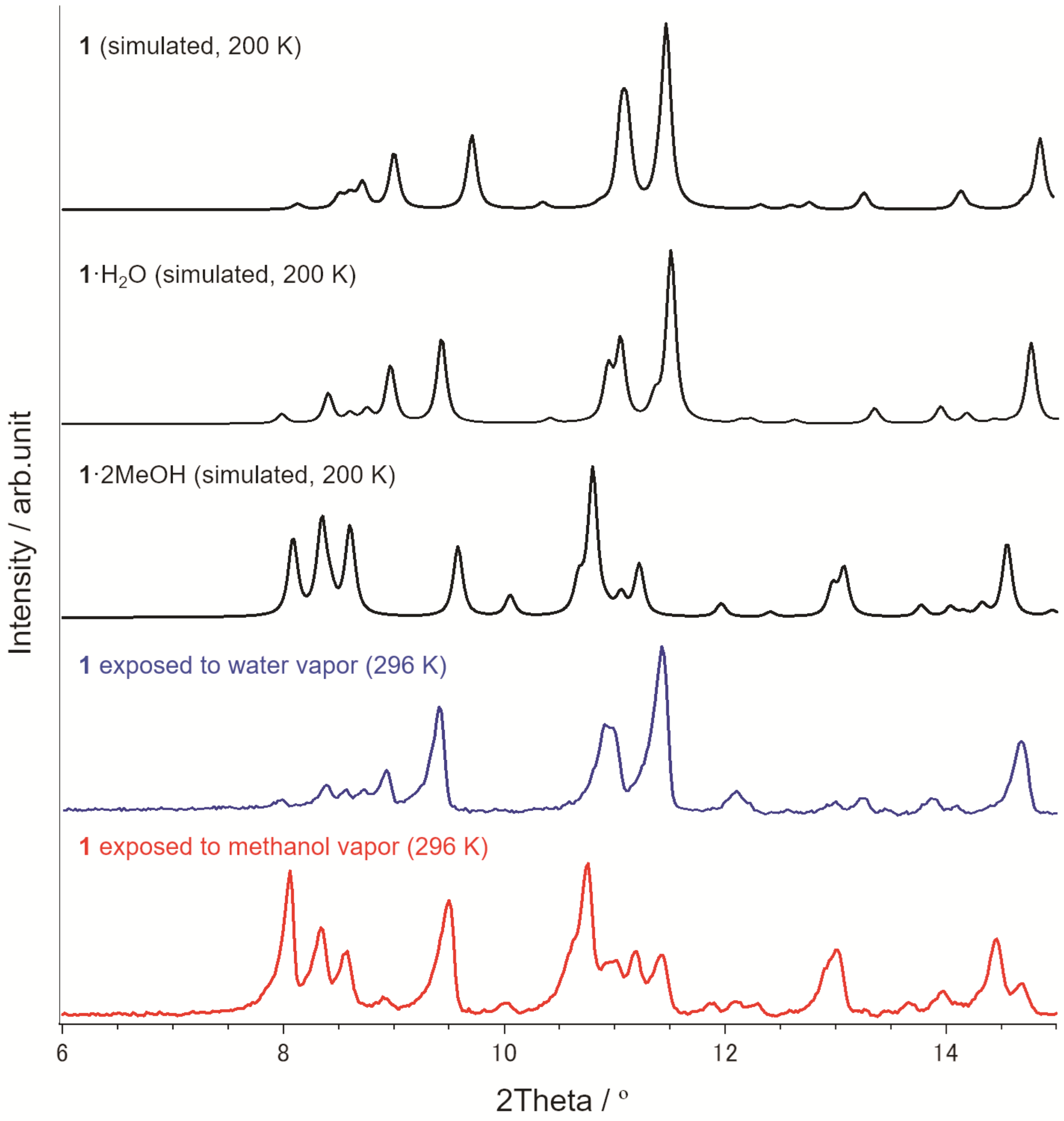

Fig. S6. PXRD patterns of polycrystalline powder of **1** exposed to water or methanol vapor, and the powder patterns of **1**·2MeOH, **1**, and **1**·H_2O simulated by the structure obtained by single-crystal XRD measurements.

UV–vis absorption spectra

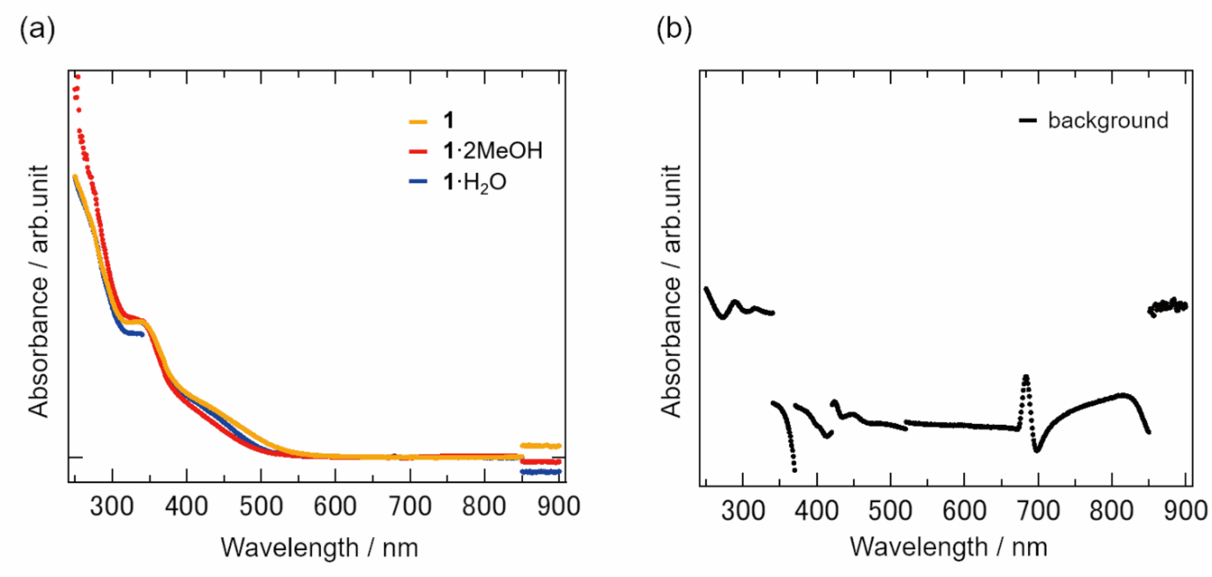

Fig. S7. (a) Full-range UV–vis absorption spectra of **1**·2MeOH, **1**, and **1**·H_2O after background subtraction. (b) Background spectrum (KBr pellet covered by liquid paraffin).

Photoluminescence spectra

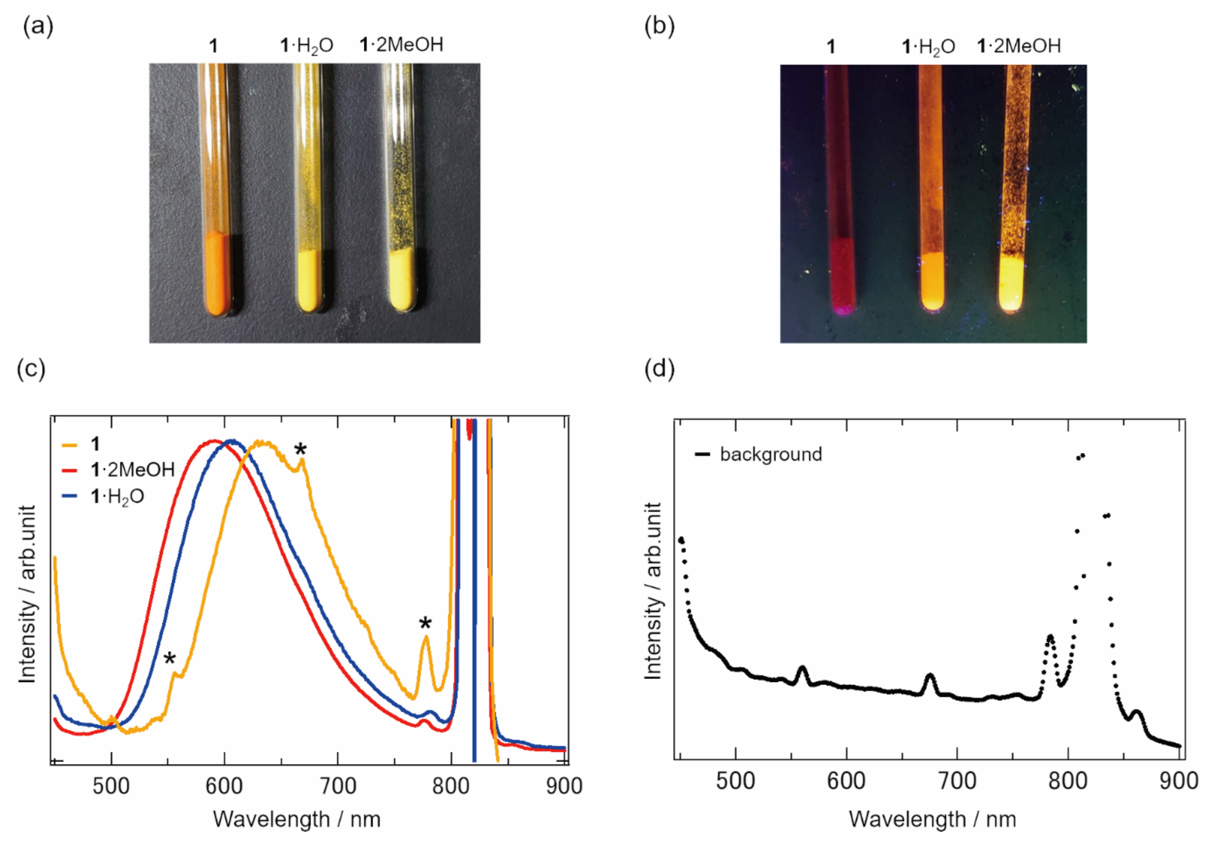

Fig. S8. (a), (b) Photographs of the samples for the photoluminescence measurements under (a) visible-light and (b) UV–light (excitation wavelength: 365 nm). (c), (d) Full range photoluminescence spectra of (c) the samples and (d) background (empty quartz glass tubes). Asterisks in (c) denote the peaks from the background, and the large peaks around 410 nm and 820 nm originate from the excitation light.

First-principles calculations

Calculations on the molecular orbitals of an isolated $[Zn(4\text{-mxbdt})_2]^{2-}$ complex molecule in **1**·2MeOH, **1**, and **1**·H_2O were carried out based on the atomic coordinates of the Zn complex in each crystal structure obtained by the single-crystal XRD measurements without structural optimization. Energies and distribution of molecular orbitals were shown in Fig. S9.

For **1**·2MeOH, we adopted the structure refined on X-ray structural analysis with the H atoms in the O–H group of the disordered MeOH-2 and MeOH-3 molecules. We confirmed that the atomic coordinates were almost the same between the cases with and without the H atoms (Supplementary files).

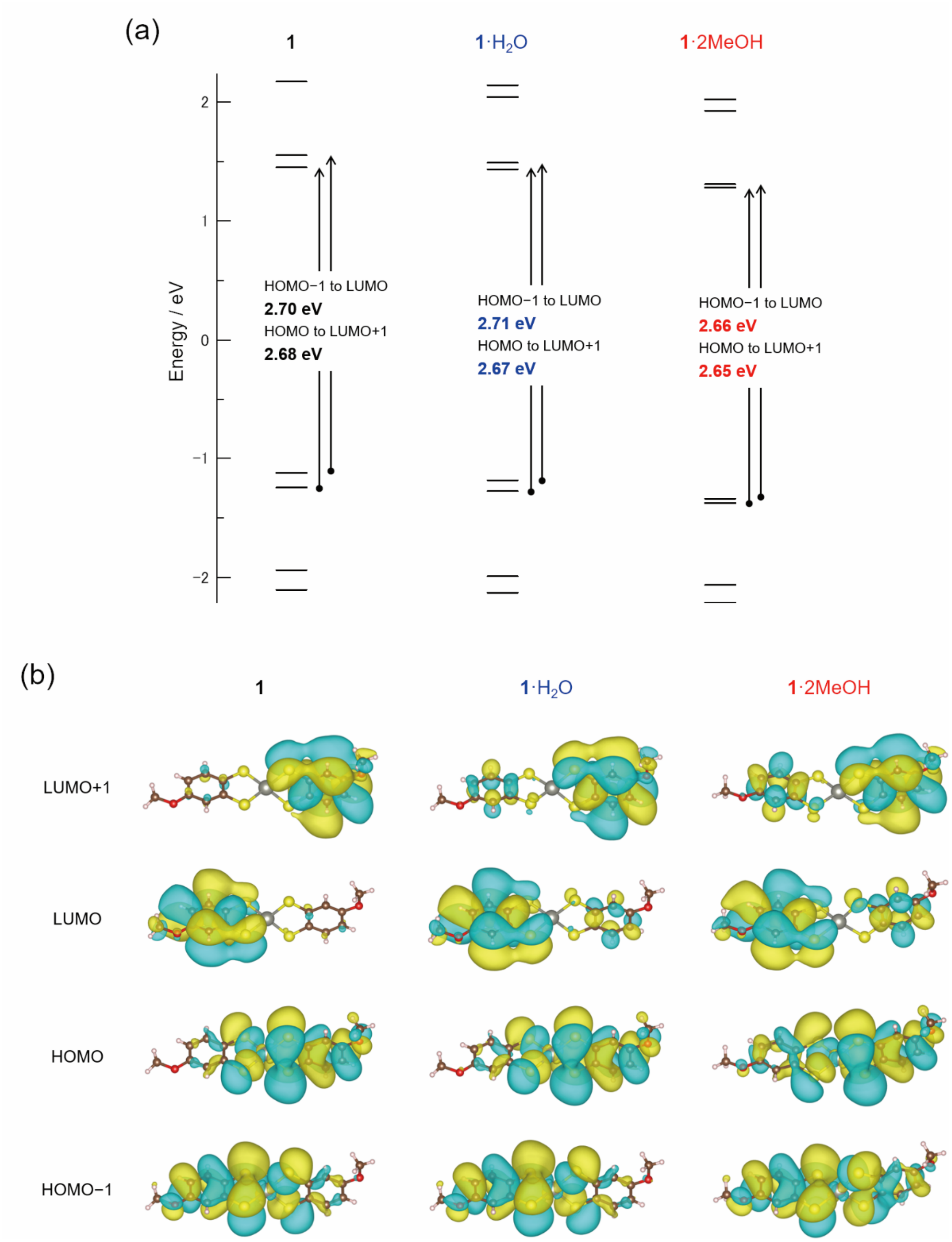

Fig. S9. (a) Energies and (b) distributions of HOMO−1, HOMO, LUMO, and LUMO+1 of an isolated $[Zn(4\text{-}mxbdt)_2]^{2-}$ complex molecule in **1**, **1**·H_2O, and **1**·2MeOH.

As shown in Fig. S9b, the distributions of HOMO-1 and HOMO were similar to LUMO and LUMO+1, respectively. As will be mentioned later, the transitions attributed to visible-light absorption correspond mainly to “HOMO−1 to LUMO” and “HOMO to LUMO+1”. The transition energies between these orbitals were 2.68–2.70 eV, 2.67–2.71 eV, and 2.65–2.66 eV for **1**, **1**$\cdot H_2O$, and **1**·2MeOH, respectively (Fig. S9a) which indicated a slight red shift, inconsistent with the experimental observations. This result clearly shows that the calculation model of an “isolated” molecule, which has often been employed to discuss the mechanism in previous research, cannot explain the observed blue shift and the mechanism of vaporochromism in these crystals. Therefore, we performed the first-principles calculations of crystal orbitals based on the experimentally observed structure, where intermolecular interactions and periodicities in the real crystalline materials are taken into account, as discussed in the main text.

Calculations of crystal orbitals and absorption spectra were carried out based on the crystal structure obtained by single-crystal XRD measurements. Note that similar to the molecular orbitals calculations, for **1**·2MeOH, we adopted the atomic coordinates refined on X-ray structural analysis with the H atoms in the O–H group of the disordered MeOH-2 and MeOH-3 molecules (Supplementary files). For the calculations, totally nine structural models were used: the actual four crystal structures obtained by the XRD measurements (**1**·2MeOH (minor), **1**·2MeOH (major), **1**, and **1**$\cdot H_2O$, where only the minor or major components of disordered methanol were considered in **1**·2MeOH (minor), **1**·2MeOH (major)), hypothetical two crystal structures without vapor molecules, obtained by removing absorbed vapor molecules from the crystals **1**$\cdot H_2O$ or **1**·2MeOH (**1**$\cdot H_2O$ without H_2O, **1**·2MeOH without 2MeOH), and hypothetical three structures consisting of only the absorbed vapor molecules in the crystal (H_2O in **1**$\cdot H_2O$, MeOH-1,2 in **1**·2MeOH (minor), and MeOH-1,3 in **1**·2MeOH (major)). Structural optimization was applied only H atoms on O atoms of MeOH-2 and MeOH-3 in **1**·2 MeOH because the positions of the H atoms could not be determined by X-ray structural analysis due to positional disorder of the methanol molecules.

In addition, the number of electrons on each atom were estimated by Mulliken population analysis.[1] In Mulliken population analysis, the occupancy of disordered methanol molecules (MeOH-2 and

MeOH-3) was assumed to be 1.00. The number of transferred electrons between $[Zn(4\text{-mxbdt})_2]^{2-}$ complex and absorbed vapor molecules was calculated from the difference between Mulliken charges calculated from the experimental crystal structure (**1**·2MeOH (major), **1**·2MeOH (minor), and **1**·H_2O) and hypothetical crystal structures (**1**·H_2O without H_2O, **1**·2MeOH (minor) without 2MeOH, and **1**·2MeOH (major) without 2MeOH) or absorbed vapor molecules in the crystal (H_2O in **1**·H_2O, MeOH-1,2 in **1**·2MeOH (minor), and MeOH-1,3 in **1**·2MeOH (major)), respectively. Also, the number of transferred electrons on each S atoms (S1 ~ S4) was calculated from differences of an average of Mulliken charges for each S atom on four crystallographically equivalent $[Zn(4\text{-mxbdt})_2]^{2-}$ complex molecules in the unit cell. The total number of transferred electrons of $[Zn(4\text{-mxbdt})_2]^{2-}$ complex and absorbed molecules was calculated from total Mulliken charges for all atoms belonging to each molecule. The Mulliken charges for each atom on the $[Zn(4\text{-mxbdt})_2]^{2-}$ complex and absorbed vapor molecules in each crystal are listed in the following tables.

Table S2. The results of Mulliken population analysis of $[Zn(4\text{-mxbdt})_2]^{2-}$ complex and vapor molecules in **1**·2MeOH (minor). Here, Mulliken charges for each atom in neutral state are as follows: Zn = 20, S = 6, O = 6, C = 4, and H = 1. The atom labels correspond to that in CIF file.

Crystal	**1**·2MeOH (minor) $[Zn(4\text{-mxbdt})_2]^{2-}$	**1**·2MeOH (minor) without 2MeOH $[Zn(4\text{-mxbdt})_2]^{2-}$	Difference
Zn1	19.68553738	19.68913075	−0.003593368
Zn1	19.68553733	19.68887914	−0.003341803
Zn1	19.6855373	19.6891308	−0.003593497
Zn1	19.68553726	19.68887911	−0.003341847
S1	6.509375276	6.513286775	−0.003911499
S1	6.509375275	6.513023147	−0.003647872
S1	6.509375329	6.513286755	−0.003911426
S1	6.509375306	6.513023168	−0.003647862
S2	6.522154644	6.532714725	−0.010560081
S2	6.52215451	6.532621143	−0.010466633
S2	6.522154861	6.532714887	−0.010560026
S2	6.522154506	6.532621153	−0.010466647
S3	6.433217809	6.526347263	−0.093129454
S3	6.433217695	6.526333597	−0.093115902
S3	6.433217592	6.526347212	−0.09312962
S3	6.433217863	6.526333746	−0.093115883
S4	6.514067918	6.521208849	−0.007140931
S4	6.514067829	6.521199831	−0.007132002
S4	6.514067923	6.521208821	−0.007140898
S4	6.514067793	6.521199782	−0.007131989
O1	6.446548809	6.448016786	−0.001467977
O1	6.446549036	6.44801	−0.001460964
O1	6.446548816	6.448016772	−0.001467956
O1	6.446549037	6.448009991	−0.001460954
O2	6.451636727	6.451547432	8.9295E-05
O2	6.451636591	6.45159612	4.0471E-05
O2	6.451636686	6.451547401	8.9285E-05
O2	6.451636684	6.451595997	4.0687E-05
C1	3.839479773	3.841588641	−0.002108868
C1	3.839479919	3.842092144	−0.002612225
C1	3.839479487	3.841588467	−0.00210898

C1	3.839479925	3.842092175	−0.00261225
C2	3.978290903	3.980240381	−0.001949478
C2	3.97829132	3.97997944	−0.00168812
C2	3.97829101	3.980240539	−0.001949529
C2	3.97829129	3.979979358	−0.001688068
H2	1.088195783	1.092702582	−0.004506799
H2	1.088196015	1.09269534	−0.004499325
H2	1.088195799	1.092702595	−0.004506796
H2	1.088196001	1.092695388	−0.004499387
C3	3.771393633	3.773463534	−0.002069901
C3	3.77139285	3.773150629	−0.001757779
C3	3.771393482	3.773463473	−0.002069991
C3	3.771392875	3.773150643	−0.001757768
C4	3.97477655	3.984823782	−0.010047232
C4	3.974775852	3.985597108	−0.010821256
C4	3.974776602	3.984823669	−0.010047067
C4	3.974775903	3.985597108	−0.010821205
H4	1.071164617	1.059938736	0.011225881
H4	1.071165082	1.059739265	0.011425817
H4	1.071164638	1.059938744	0.011225894
H4	1.071165032	1.059739303	0.011425729
C5	3.924674265	3.925644744	−0.000970479
C5	3.924674491	3.92613997	−0.001465479
C5	3.92467452	3.925645013	−0.000970493
C5	3.924674613	3.926139877	−0.001465264
H5	1.067992012	1.068348355	−0.000356343
H5	1.06799184	1.068131261	−0.000139421
H5	1.067991643	1.068348087	−0.000356444
H5	1.067991787	1.068131306	−0.000139519
C6	3.853767872	3.858344285	−0.004576413
C6	3.853768108	3.858210591	−0.004442483
C6	3.85376805	3.858344312	−0.004576262
C6	3.853768059	3.858210603	−0.004442544
C7	3.828375227	3.862091302	−0.033716075
C7	3.828375333	3.862078509	−0.033703176
C7	3.828375485	3.862091533	−0.033716048
C7	3.828374888	3.862078012	−0.033703124
C8	3.917103812	3.938935999	−0.021832187

C8	3.917103531	3.938833008	−0.021729477
C8	3.917103591	3.938935801	−0.02183221
C8	3.917103964	3.938833811	−0.021729847
H8	1.080140904	1.076515537	0.003625367
H8	1.080141349	1.076584627	0.003556722
H8	1.080141512	1.076516193	0.003625319
H8	1.080141252	1.076584664	0.003556588
C9	3.747284314	3.753864793	−0.006580479
C9	3.747284761	3.75383584	−0.006551079
C9	3.747283577	3.753863929	−0.006580352
C9	3.747284039	3.753835845	−0.006551806
C10	4.001905014	4.012154382	−0.010249368
C10	4.001905044	4.012224356	−0.010319312
C10	4.001905216	4.012154607	−0.010249391
C10	4.001905313	4.012223949	−0.010318636
H10	1.073473955	1.080195608	−0.006721653
H10	1.073473773	1.08020853	−0.006734757
H10	1.073473933	1.080195653	−0.00672172
H10	1.073473619	1.080208068	−0.006734449
C11	3.919895379	3.931332064	−0.011436685
C11	3.919895277	3.931260956	−0.011365679
C11	3.919895514	3.931331935	−0.011436421
C11	3.919895593	3.93126149	−0.011365897
H11	1.056633341	1.052297578	0.004335763
H11	1.056633443	1.052279114	0.004354329
H11	1.056633315	1.052297623	0.004335692
H11	1.056633412	1.052279123	0.004354289
C12	3.852664465	3.860436448	−0.007771983
C12	3.852664284	3.860463076	−0.007798792
C12	3.852664354	3.860436467	−0.007772113
C12	3.852664314	3.860463109	−0.007798795
C13	3.72961643	3.738955125	−0.009338695
C13	3.729616232	3.738926514	−0.009310282
C13	3.729615892	3.738954611	−0.009338719
C13	3.729616203	3.738926584	−0.009310381
H13A	1.022272329	1.020967657	0.001304672
H13A	1.022272691	1.020950556	0.001322135
H13A	1.022272299	1.020967633	0.001304666

H13A	1.022272752	1.020950524	0.001322228
H13B	1.019070215	1.018021573	0.001048642
H13B	1.019070615	1.018056266	0.001014349
H13B	1.019070861	1.018022172	0.001048689
H13B	1.0190706	1.018056211	0.001014389
H13C	0.984716611	0.977971384	0.006745227
H13C	0.984715983	0.978019361	0.006696622
H13C	0.984716505	0.977971334	0.006745171
H13C	0.984715972	0.978019383	0.006696589
C14	3.744276018	3.758512059	−0.014236041
C14	3.744275874	3.759204984	−0.01492911
C14	3.744276606	3.758512695	−0.014236089
C14	3.744276655	3.759204582	−0.014927927
H14A	1.008153344	1.010354146	−0.002200802
H14A	1.008153391	1.010597926	−0.002444535
H14A	1.008152794	1.010353605	−0.002200811
H14A	1.008153249	1.010598002	−0.002444753
H14B	1.021724606	1.028734368	−0.007009762
H14B	1.021724992	1.027412887	−0.005687895
H14B	1.021724768	1.028734479	−0.007009711
H14B	1.021724762	1.02741302	−0.005688258
H14C	0.985128418	0.97030733	0.014821088
H14C	0.985127917	0.97052932	0.014598597
H14C	0.985128233	0.970307156	0.014821077
H14C	0.985127748	0.970529504	0.014598244
Crystal	**1**·2MeOH (minor)	MeOH in **1**·2MeOH (minor)	
	MeOH-1	MeOH-1	Difference
O3	6.602273169	6.621176692	−0.018903523
O3	6.602273322	6.621183676	−0.018910354
O3	6.602273163	6.621178428	−0.018905265
O3	6.602273028	6.621183645	−0.018910617
H3	0.770678062	0.660520213	0.110157849
H3	0.770677866	0.660513822	0.110164044
H3	0.770678079	0.660518833	0.110159246
H3	0.770678174	0.660513352	0.110164822
C63	3.713456326	3.776465546	−0.06300922
C63	3.713456503	3.776467348	−0.063010845
C63	3.713456336	3.77646533	−0.063008994

C63	3.713456508	3.776463731	−0.063007223
H63A	1.015835102	0.975149471	0.040685631
H63A	1.015835435	0.975142873	0.040692562
H63A	1.015835115	0.975149255	0.04068586
H63A	1.015835135	0.975141825	0.04069331
H63B	0.991151858	0.964558384	0.026593474
H63B	0.991151562	0.964564506	0.026587056
H63B	0.991151826	0.964558534	0.026593292
H63B	0.991151572	0.964563944	0.026587628
H63C	1.013810063	1.00312756	0.010682503
H63C	1.013809989	1.003125706	0.010684283
H63C	1.013810075	1.00312749	0.010682585
H63C	1.013810177	1.003131447	0.01067873
	MeOH-2	MeOH-2	Difference
O4	6.530319638	6.545956973	−0.015637335
O4	6.530319796	6.545959442	−0.015639646
O4	6.530319464	6.545957062	−0.015637598
O4	6.530319033	6.545959464	−0.015640431
H4A	0.8682202	0.736628634	0.131591566
H4A	0.868219766	0.736624853	0.131594913
H4A	0.868219939	0.736628463	0.131591476
H4A	0.868220484	0.736624849	0.131595635
C65A	3.710764837	3.787279585	−0.076514748
C65A	3.710764937	3.787279603	−0.076514666
C65A	3.710765794	3.787279869	−0.076514075
C65A	3.710765367	3.787279519	−0.076514152
H65A	1.025560173	0.988939601	0.036620572
H65A	1.025560392	0.988937097	0.036623295
H65A	1.025560299	0.988939696	0.036620603
H65A	1.025560278	0.988937146	0.036623132
H65B	1.018076917	0.983543661	0.034533256
H65B	1.018076824	0.983552947	0.034523877
H65B	1.018076655	0.983543759	0.034532896
H65B	1.018076698	0.983552975	0.034523723
H65C	0.988725746	0.956653677	0.032072069
H65C	0.988725712	0.956648113	0.032077599
H65C	0.988725378	0.956653282	0.032072096
H65C	0.988725678	0.956648115	0.032077563

Table S3. The results of Mulliken population analysis of $[\mathrm{Zn(4\text{-}mxbdt)_2}]^{2-}$ complex and vapor molecules in **1**·2MeOH (major). Here, Mulliken charges for each atom in neutral state are as follows: Zn = 20, S = 6, O = 6, C = 4, and H = 1. The atom labels correspond to that in CIF file.

Crystal	**1**·2MeOH (major)	**1**·2MeOH (major) without 2MeOH	
	$[\mathrm{Zn(4\text{-}mxbdt)_2}]^{2-}$	$[\mathrm{Zn(4\text{-}mxbdt)_2}]^{2-}$	Difference
Zn1	19.68216665	19.68913075	−0.006964105
Zn1	19.68216743	19.68887914	−0.006711702
Zn1	19.68216727	19.6891308	−0.006963529
Zn1	19.68216725	19.68887911	−0.006711861
S1	6.505559352	6.513286775	−0.007727423
S1	6.50556001	6.513023147	−0.007463137
S1	6.505559895	6.513286755	−0.00772686
S1	6.505559897	6.513023168	−0.007463271
S2	6.469401987	6.532714725	−0.063312738
S2	6.469406312	6.532621143	−0.063214831
S2	6.469405856	6.532714887	−0.063309031
S2	6.469405739	6.532621153	−0.063215414
S3	6.476255219	6.526347263	−0.050092044
S3	6.476256235	6.526333597	−0.050077362
S3	6.476255969	6.526347212	−0.050091243
S3	6.476256316	6.526333746	−0.05007743
S4	6.518213909	6.521208849	−0.00299494
S4	6.518213838	6.521199831	−0.002985993
S4	6.518213935	6.521208821	−0.002994886
S4	6.518213743	6.521199782	−0.002986039
O1	6.443044951	6.448016786	−0.004971835
O1	6.443045137	6.448010000	−0.004964863
O1	6.44304496	6.448016772	−0.004971812
O1	6.443045184	6.448009991	−0.004964807
O2	6.452320053	6.451547432	0.000772621
O2	6.452320043	6.45159612	0.000723923
O2	6.452320138	6.451547401	0.000772737
O2	6.452320058	6.451595997	0.000724061
C1	3.840889493	3.841588641	−0.000699148
C1	3.840890063	3.842092144	−0.001202081
C1	3.840889569	3.841588467	−0.000698898

C1	3.840889949	3.842092175	−0.001202226
C2	3.977452841	3.980240381	−0.00278754
C2	3.977453476	3.979979440	−0.002525964
C2	3.977453082	3.980240539	−0.002787457
C2	3.977453424	3.979979358	−0.002525934
H2	1.090762771	1.092702582	−0.001939811
H2	1.090763225	1.09269534	−0.001932115
H2	1.090762931	1.092702595	−0.001939664
H2	1.090763144	1.092695388	−0.001932244
C3	3.766044622	3.773463534	−0.007418912
C3	3.766044354	3.773150629	−0.007106275
C3	3.766044986	3.773463473	−0.007418487
C3	3.766044413	3.773150643	−0.00710623
C4	3.969946757	3.984823782	−0.014877025
C4	3.969946	3.985597108	−0.015651108
C4	3.969946896	3.984823669	−0.014876773
C4	3.969946185	3.985597108	−0.015650923
H4	1.062494663	1.059938736	0.002555927
H4	1.062495096	1.059739265	0.002755831
H4	1.062494756	1.059938744	0.002556012
H4	1.062495241	1.059739303	0.002755938
C5	3.922852138	3.925644744	−0.002792606
C5	3.922852663	3.92613997	−0.003287307
C5	3.922852572	3.925645013	−0.002792441
C5	3.922852631	3.926139877	−0.003287246
H5	1.066366436	1.068348355	−0.001981919
H5	1.066366474	1.068131261	−0.001764787
H5	1.066366346	1.068348087	−0.001981741
H5	1.066366468	1.068131306	−0.001764838
C6	3.831253723	3.858344285	−0.027090562
C6	3.831255502	3.858210591	−0.026955089
C6	3.831255184	3.858344312	−0.027089128
C6	3.831255246	3.858210603	−0.026955357
C7	3.838290509	3.862091302	−0.023800793
C7	3.838290538	3.862078509	−0.023787971
C7	3.838290641	3.862091533	−0.023800892
C7	3.838290259	3.862078012	−0.023787753
C8	3.920082959	3.938935999	−0.01885304

C8	3.92008275	3.938833008	−0.018750258
C8	3.920082871	3.938935801	−0.01885293
C8	3.920083104	3.938833811	−0.018750707
H8	1.083454443	1.076515537	0.006938906
H8	1.083454936	1.076584627	0.006870309
H8	1.083455128	1.076516193	0.006938935
H8	1.083454869	1.076584664	0.006870205
C9	3.749273371	3.753864793	−0.004591422
C9	3.749273759	3.75383584	−0.004562081
C9	3.749272595	3.753863929	−0.004591334
C9	3.749273124	3.753835845	−0.004562721
C10	4.005059645	4.012154382	−0.007094737
C10	4.005059823	4.012224356	−0.007164533
C10	4.005059747	4.012154607	−0.00709486
C10	4.005060106	4.012223949	0.007163843
H10	1.075539311	1.080195608	0.004656297
H10	1.075539239	1.08020853	0.004669291
H10	1.075539462	1.080195653	0.004656191
H10	1.075538992	1.080208068	0.004669076
C11	3.921071606	3.931332064	0.010260458
C11	3.921071318	3.931260956	0.010189638
C11	3.921071353	3.931331935	0.010260582
C11	3.921071639	3.93126149	0.010189851
H11	1.058041332	1.052297578	0.005743754
H11	1.058041508	1.052279114	0.005762394
H11	1.058041482	1.052297623	0.005743859
H11	1.05804146	1.052279123	0.005762337
C12	3.853763592	3.860436448	−0.006672856
C12	3.853763521	3.860463076	−0.006699555
C12	3.853763663	3.860436467	−0.006672804
C12	3.85376342	3.860463109	−0.006699689
C13	3.729425207	3.738955125	−0.009529918
C13	3.729425207	3.738926514	−0.009501307
C13	3.729424744	3.738954611	−0.009529867
C13	3.72942512	3.738926584	−0.009501464
H13A	1.021411825	1.020967657	0.000444168
H13A	1.021412274	1.020950556	0.000461718
H13A	1.021411782	1.020967633	0.000444149

H13A	1.021412272	1.020950524	0.000461748
H13B	1.023934267	1.018021573	0.005912694
H13B	1.023934847	1.018056266	0.005878581
H13B	1.023935136	1.018022172	0.005912964
H13B	1.023934838	1.018056211	0.005878627
H13C	0.981058934	0.977971384	0.00308755
H13C	0.981058595	0.978019361	0.003039234
H13C	0.981059096	0.977971334	0.003087762
H13C	0.981058564	0.978019383	0.003039181
C14	3.744717157	3.758512059	–0.013794902
C14	3.744716955	3.759204984	–0.014488029
C14	3.744717645	3.758512695	–0.01379505
C14	3.744717841	3.759204582	–0.014486741
H14A	1.00785272	1.010354146	–0.002501426
H14A	1.007852734	1.010597926	–0.002745192
H14A	1.007852219	1.010353605	–0.002501386
H14A	1.00785261	1.010598002	–0.002745392
H14B	1.022380892	1.028734368	–0.006353476
H14B	1.022381364	1.027412887	–0.005031523
H14B	1.022381103	1.028734479	–0.006353376
H14B	1.02238108	1.02741302	–0.00503194
H14C	0.986433951	0.97030733	0.016126621
H14C	0.986433469	0.97052932	0.015904149
H14C	0.986433732	0.970307156	0.016126576
H14C	0.986433285	0.970529504	0.015903781

Crystal	**1**·2MeOH (major)	MeOH in **1**·2MeOH (major)	
	MeOH-1	MeOH-1	Difference
O3	6.602609432	6.62267698	–0.020067548
O3	6.60260959	6.622683903	–0.020074313
O3	6.602609445	6.622678665	–0.02006922
O3	6.602609315	6.62268386	–0.020074545
H3	0.771091244	0.656161968	0.114929276
H3	0.771091026	0.656155648	0.114935378
H3	0.771091261	0.656160677	0.114930584
H3	0.771091294	0.656155188	0.114936106
C63	3.714730594	3.777139478	–0.062408884
C63	3.714730788	3.777141202	–0.062410414
C63	3.71473064	3.777139251	–0.062408611

C63	3.714730746	3.777137649	−0.062406903
H63A	1.014813216	0.973740328	0.041072888
H63A	1.014813543	0.973733667	0.041079876
H63A	1.014813184	0.973740093	0.041073091
H63A	1.014813187	0.973732585	0.041080602
H63B	0.991391344	0.965505660	0.025885684
H63B	0.991391031	0.965511739	0.025879292
H63B	0.991391366	0.965505747	0.025885619
H63B	0.991391111	0.965511158	0.025879953
H63C	1.017190488	1.004843646	0.012346842
H63C	1.017190387	1.004841917	0.01234847
H63C	1.017190437	1.004843627	0.01234681
H63C	1.017190504	1.004847633	0.012342871
	MeOH-3	MeOH-3	Difference
O5	6.527360032	6.544926663	−0.017566631
O5	6.527345555	6.544911991	−0.017566436
O5	6.527358547	6.544924538	−0.017565991
O5	6.52735781	6.544927794	−0.017569984
H5A	0.874450342	0.734422083	0.140028259
H5A	0.874473404	0.734437337	0.140036067
H5A	0.874452865	0.73442465	0.140028215
H5A	0.874454658	0.734420198	0.14003446
C65B	3.728446369	3.793681380	−0.065235011
C65B	3.728446043	3.793677455	−0.065231412
C65B	3.728446314	3.793680898	−0.065234584
C65B	3.728445285	3.793680166	−0.065234881
H65D	0.994414447	0.95527323	0.039141217
H65D	0.994415529	0.955272323	0.039143206
H65D	0.99441493	0.955273214	0.039141716
H65D	0.994414627	0.955272782	0.039141845
H65E	1.023324584	0.987149203	0.036175381
H65E	1.023324738	0.987138115	0.036186623
H65E	1.023324028	0.987149087	0.036174941
H65E	1.023324011	0.98713756	0.036186451
H65F	1.01290286	0.984479381	0.028423479
H65F	1.012905356	0.984494706	0.02841065
H65F	1.012903348	0.984479551	0.028423797
H65F	1.012904226	0.984493426	0.0284108

Table S4. The results of Mulliken population analysis of $[Zn(4\text{-}mxbdt)_2]^{2-}$ complex and vapor molecules in **1**·H_2O. Here, Mulliken charges for each atom in neutral state are as follows: Zn = 20, S = 6, O = 6, C = 4, and H = 1. The atom labels correspond to that in CIF file.

Crystal	**1**·H_2O	**1**·H_2O without H_2O	
	$[Zn(4\text{-}mxbdt)_2]^{2-}$	$[Zn(4\text{-}mxbdt)_2]^{2-}$	Difference
Zn1	19.69261456	19.70000716	−0.007392606
Zn1	19.69261454	19.70000973	−0.007395197
Zn1	19.69261692	19.70000713	−0.007390208
Zn1	19.6926169	19.7000097	−0.007392799
S1	6.517221222	6.520103659	−0.002882437
S1	6.517221253	6.520153571	−0.002932318
S1	6.517271141	6.520103687	−0.002832546
S1	6.517271238	6.520153669	−0.002882431
S2	6.485295353	6.537784411	−0.052489058
S2	6.485295258	6.537763616	−0.052468358
S2	6.485273166	6.537784317	−0.052511151
S2	6.485273136	6.537763615	−0.052490479
S3	6.480131539	6.526811038	−0.046679499
S3	6.480131645	6.526732317	−0.046600672
S3	6.480046617	6.526811101	−0.046764484
S3	6.48004643	6.526732114	−0.046685684
S4	6.549923731	6.555898083	−0.005974352
S4	6.549923669	6.555844204	−0.005920535
S4	6.549869957	6.555898023	−0.006028066
S4	6.549869868	6.555844116	−0.005974248
O1	6.448365804	6.449245916	−0.000880112
O1	6.448365905	6.449394674	−0.001028769
O1	6.448515282	6.449246015	−0.000730733
O1	6.448515368	6.449394757	−0.000879389
O2	6.448948016	6.449137139	−0.000189123
O2	6.448948106	6.449051925	−0.000103819
O2	6.448862427	6.44913723	−0.000274803
O2	6.448862553	6.449052054	−0.000189501
C1	3.840814461	3.844057162	−0.003242701
C1	3.840814816	3.843960570	−0.003145754
C1	3.84071746	3.844057520	−0.00334006

C1	3.840717752	3.843960866	−0.003243114
C2	3.994563239	3.997888080	−0.003324841
C2	3.994563654	3.997871622	−0.003307968
C2	3.994545259	3.997888495	−0.003343236
C2	3.99454544	3.997871807	−0.003326367
H2	1.072391461	1.075439711	−0.00304825
H2	1.072391245	1.075505287	−0.003114042
H2	1.07245391	1.075439485	−0.002985575
H2	1.072453819	1.075505191	−0.003051372
C3	3.760865642	3.765559020	−0.004693378
C3	3.760864879	3.765382816	−0.004517937
C3	3.760688626	3.765558267	−0.004869641
C3	3.760688024	3.765382215	−0.004694191
C4	3.97266042	3.976278957	−0.003618537
C4	3.972660375	3.976301512	−0.003641137
C4	3.972682222	3.976278921	−0.003596699
C4	3.972681486	3.976300798	−0.003619312
H4	1.081987124	1.084814587	−0.002827463
H4	1.081987655	1.084815151	−0.002827496
H4	1.08198748	1.084815116	−0.002827636
H4	1.081987751	1.084815412	−0.002827661
C5	3.958841797	3.961629587	−0.00278779
C5	3.958841427	3.961673336	−0.002831909
C5	3.958884988	3.961629224	−0.002744236
C5	3.958885437	3.961673783	−0.002788346
H5	1.042977198	1.044977298	−0.0020001
H5	1.042977151	1.044920148	−0.001942997
H5	1.042920261	1.044977249	−0.002056988
H5	1.042920212	1.044920093	−0.001999881
C6	3.844567993	3.854649473	−0.01008148
C6	3.844568124	3.854638457	−0.010070333
C6	3.844563051	3.854649583	−0.010086532
C6	3.844563184	3.854638558	−0.010075374
C7	3.870014892	3.872586887	−0.002571995
C7	3.870014667	3.872563175	−0.002548508
C7	3.86999045	3.872586653	−0.002596203
C7	3.869990678	3.872563394	−0.002572716
C8	3.95614155	3.957257589	−0.001116039

C8	3.956141886	3.957285214	−0.001143328
C8	3.956169114	3.957257928	−0.001088814
C8	3.956168755	3.957284857	−0.001116102
H8	1.026338817	1.028033276	−0.001694459
H8	1.026338816	1.028020856	−0.00168204
H8	1.026326705	1.028033269	−0.001706564
H8	1.026326708	1.028020859	−0.001694151
C9	4.041928274	4.045361590	−0.003433316
C9	4.041928293	4.045351653	−0.00342336
C9	4.04191825	4.045361606	−0.003443356
C9	4.041917948	4.045351352	−0.003433404
C10	1.047733199	1.049894406	−0.002161207
C10	1.047733022	1.049903016	−0.002169994
C10	1.047741843	1.049894234	−0.002152391
C10	1.047742105	1.049903283	−0.002161178
H10	3.763743022	3.765649406	−0.001906384
H10	3.76374303	3.765710062	−0.001967032
H10	3.763804324	3.765649402	−0.001845078
H10	3.763804355	3.765710087	−0.001905732
C11	3.941212502	3.943902271	−0.002689769
C11	3.941212571	3.943869452	−0.002656881
C11	3.941179002	3.943902353	−0.002723351
C11	3.941179517	3.943869962	−0.002690445
H11	1.060991383	1.061370489	−0.000379106
H11	1.060991662	1.061399932	−0.00040827
H11	1.061021290	1.061370768	−0.000349478
H11	1.061021189	1.061399832	−0.000378643
C12	3.853006691	3.863229065	−0.010222374
C12	3.853006273	3.863259925	−0.010253652
C12	3.853040281	3.863228658	−0.010188377
C12	3.853040193	3.863259827	−0.010219634
C13	3.770089033	3.776198360	−0.006109327
C13	3.770088974	3.776292699	−0.006203725
C13	3.770182500	3.776198293	−0.006015793
C13	3.770182257	3.776292466	−0.006110209
H13A	1.005050418	1.007655179	−0.002604761
H13A	1.005050566	1.007646153	−0.002595587
H13A	1.005041479	1.007655325	−0.002613846

H13A	1.005041896	1.007646565	−0.002604669
H13B	1.004485900	1.005144816	−0.000658916
H13B	1.004485594	1.005136929	−0.000651335
H13B	1.004477842	1.005144510	−0.000666668
H13B	1.004477592	1.005136679	−0.000659087
H13C	0.970130273	0.969586298	0.000543975
H13C	0.970130489	0.969592633	0.000537856
H13C	0.970135529	0.969586523	0.000549006
H13C	0.970135589	0.969592687	0.000542902
C14	3.787807140	3.788348750	−0.00054161
C14	3.787807309	3.788386134	−0.000578825
C14	3.787844555	3.788348911	−0.000504356
C14	3.787844205	3.788385794	−0.000541589
H14A	0.988711104	0.988695704	1.54E-05
H14A	0.988711141	0.988667981	4.316E-05
H14A	0.988683514	0.988695746	−1.2232E-05
H14A	0.98868349	0.988667949	1.5541E-05
H14B	0.992028638	0.994021477	−0.001992839
H14B	0.992028614	0.994071468	−0.002042854
H14B	0.992078469	0.994021451	−0.001942982
H14B	0.99207864	0.994071639	-0.001992999
H14C	0.960809403	0.960576594	0.000232809
H14C	0.960809200	0.960526577	0.000282623
H14C	0.960759221	0.960576396	0.000182825
H14C	0.960759396	0.960526747	0.000232649

Crystal	**1**·H_2O	H_2O in **1**·H_2O	
	H_2O	H_2O	Difference
O3	6.684782278	6.711115053	−0.026332775
O3	6.684782209	6.711045831	−0.026263622
O3	6.684715938	6.711114968	−0.02639903
O3	6.684715845	6.711045740	−0.026329895
H1	0.768767070	0.639402917	0.129364153
H1	0.768766776	0.639535079	0.129231697
H1	0.768884065	0.639402856	0.129481209
H1	0.768883751	0.639535017	0.129348734
H3	0.751191464	0.649482030	0.101709434
H3	0.751191809	0.649419090	0.101772719
H3	0.751148416	0.649482176	0.10166624

H3	0.751148759	0.649419243	0.101729516

The intensities of absorption in the crystals were estimated from an average of diagonal terms of the absorption coefficient tensor, α_{xx}, α_{yy}, and α_{zz}. The crystal orbitals related to visible-light absorption in each crystal were determined by comparison of a real part of the optical conductivity ($\propto$ absorption coefficient) resolved for each k point and crystal orbital pair. The unit cells are sufficiently large so that interactions of each crystal orbital among unit cells are small. Thus, calculated absorption spectra can be attributed by just considering transitions between crystal orbitals at Γ point. In this case, the intensity of the absorption spectra is proportional to the magnitude of a real part of the optical conductivity, and we need to consider only the real part of the wave functions. The crystal orbital pairs for the transitions contributed to visible-light absorption peaks (around 3.0 eV) and optical conductivities in order of the magnitude are listed in the following tables.

Table S5. Optical conductivities of transitions between crystal orbitals attributed to visible-light absorption in **1** at 2.86 eV and 2.98 eV.

Occupied orbital	Unoccupied orbital	Optical conductivity (a. u.)	Energy difference (eV)
725 (HOCO−7)	798 (LUCO+65)	226.28125	2.852
727 (HOCO−5)	800 (LUCO+67)	225.92794	2.855
728 (HOCO−4)	799 (LUCO+66)	225.09436	2.848
726 (HOCO−6)	797 (LUCO+64)	213.73490	2.845
732 (HOCO)	802 (LUCO+69)	44.13738	2.957
730 (HOCO−2)	803 (LUCO+70)	34.11675	2.974
732 (HOCO)	801 (LUCO+68)	25.84606	2.921
731 (HOCO−1)	804 (LUCO+71)	21.84523	3.007
731 (HOCO−1)	803 (LUCO+70)	11.18381	2.963
730 (HOCO−2)	803 (LUCO+70)	205.16868	2.974
732 (HOCO)	802 (LUCO+69)	166.19948	2.957
731 (HOCO−2)	804 (LUCO+71)	163.56431	3.007
729 (HOCO−3)	801 (LUCO+68)	114.40408	2.939
731 (HOCO−2)	803 (LUCO+70)	51.01095	2.963
729 (HOCO−3)	802 (LUCO+69)	49.41313	2.975
730 (HOCO−2)	804 (LUCO+71)	29.79251	3.019
727 (HOCO−5)	800 (LUCO+67)	28.66196	2.855
725 (HOCO−7)	798 (LUCO+65)	28.18978	2.852
728 (HOCO−4)	799 (LUCO+66)	27.22174	2.848
726 (HOCO−6)	797 (LUCO+64)	25.67065	2.845
732 (HOCO)	801 (LUCO+68)	25.43513	2.921

Table S6. Optical conductivities of transitions between crystal orbitals attributed to visible-light absorption in **1**·H_2O at 3.01 eV.

Occupied orbital	Unoccupied orbital	Optical conductivity (a. u.)	Energy difference (eV)
744 (HOCO−4)	816 (LUCO+67)	258.80978	3.005
742 (HOCO−6)	814 (LUCO+65)	258.66819	3.004
741 (HOCO−7)	813 (LUCO+64)	257.89262	3.005
743 (HOCO−5)	815 (LUCO+66)	250.66973	3.002
747 (HOCO−1)	820 (LUCO+71)	203.93718	3.010
746 (HOCO−2)	818 (LUCO+69)	145.42868	2.984
748 (HOCO)	819 (LUCO+70)	126.10082	2.976
745 (HOCO−3)	817 (LUCO+68)	89.49873	2.960
745 (HOCO−3)	819 (LUCO+70)	37.76301	2.990
746 (HOCO−2)	820 (LUCO+71)	36.37202	3.019
747 (HOCO−1)	818 (LUCO+69)	29.41311	2.974
748 (HOCO)	817 (LUCO+68)	20.02089	2.947

Table S7. Optical conductivities of transitions between crystal orbitals attributed to visible-light absorption in **1**·2MeOH (minor) at 2.95 eV.

Occupied orbital	Unoccupied orbital	Optical conductivity (a. u.)	Energy difference (eV)
787 (HOCO−1)	860 (LUCO+71)	188.25389	2.934
784 (HOCO−4)	856 (LUCO+67)	182.12966	2.944
783 (HOCO−5)	855 (LUCO+66)	168.92545	2.943
788 (HOCO)	859 (LUCO+70)	157.51822	2.922
786 (HOCO−2)	858 (LUCO+69)	145.88360	2.923
781 (HOCO−7)	853 (LUCO+64)	139.76743	2.944
785 (HOCO−3)	857 (LUCO+68)	126.78361	2.914
782 (HOCO−6)	854 (LUCO+65)	126.42786	2.953
786 (HOCO−2)	860 (LUCO+71)	20.95589	2.936
785 (HOCO−3)	859 (LUCO+70)	17.72998	2.927
787 (HOCO−1)	858 (LUCO+69)	16.58588	2.921
788 (HOCO)	857 (LUCO+68)	12.83607	2.909
782 (HOCO−6)	856 (LUCO+67)	12.56533	2.954
781 (HOCO−7)	857 (LUCO+68)	11.89809	3.020
782 (HOCO−6)	858 (LUCO+69)	11.45663	3.027
781 (HOCO−7)	855 (LUCO+66)	10.65922	2.957
781 (HOCO−7)	855 (LUCO+66)	10.65922	2.957

Table S8. Optical conductivities of transitions between crystal orbitals attributed to visible-light absorption in **1**·2MeOH (major) at 3.03 eV.

Occupied orbital	Unoccupied orbital	Optical conductivity (a.u.)	Energy difference (eV)
783 (HOCO−5)	856 (LUCO+67)	236.26513	3.031
784 (HOCO−4)	855 (LUCO+66)	229.17454	3.020
781 (HOCO−7)	853 (LUCO+64)	224.44498	3.017
782 (HOCO−6)	854 (LUCO+65)	224.34837	3.020
786 (HOCO−2)	860 (LUCO+71)	133.77633	3.000
787 (HOCO−1)	859 (LUCO+70)	121.68839	2.987
788 (HOCO)	858 (LUCO+69)	113.67270	2.985
785 (HOCO−3)	857 (LUCO+68)	110.85168	2.988
782 (HOCO−6)	856 (LUCO+67)	41.39571	3.036
781 (HOCO−7)	855 (LUCO+66)	40.26094	3.029
783 (HOCO−5)	854 (LUCO+65)	38.37522	3.016
784 (HOCO−4)	853 (LUCO+64)	34.57263	3.008
786 (HOCO−2)	859 (LUCO+70)	17.64467	2.996
785 (HOCO−3)	858 (LUCO+69)	17.35995	2.996

Here, due to the existence of the crystallographically equivalent four $[Zn(4\text{-mxbdt})_2]^{2-}$ complexes, four crystal orbitals having almost the same distributions and energy levels degenerated. We named each four-fold degenerated crystal orbital groups as crystal orbital groups α, β, γ, and δ in order of increasing energy level of **1**. The energies of each crystal orbital group are estimated from the average of the four crystal orbital energies (Table S9). Considering this degeneracy, the transitions listed above are attributed to two kinds of transitions between the same crystal orbital groups: α to γ and β to δ.

Differential electron density maps, that show the degree of electron transfer caused by the formation of H-bonds, were drawn by subtracting the sum of the total electron density of the hypothetical crystal structure ("**1**·H_2O without H_2O", "**1**·2MeOH (minor) without 2MeOH" or "**1**·2MeOH (major) without 2MeOH") and absorbed molecules in the crystals ("H_2O in **1**·H_2O", "MeOH-1,2 in **1**·2MeOH (minor)" or "MeOH-1,3 in **1**·2MeOH (major)") from the total electron density of the actual crystal structure (**1**·H_2O, **1**·2MeOH (minor), or **1**·2MeOH (major)).

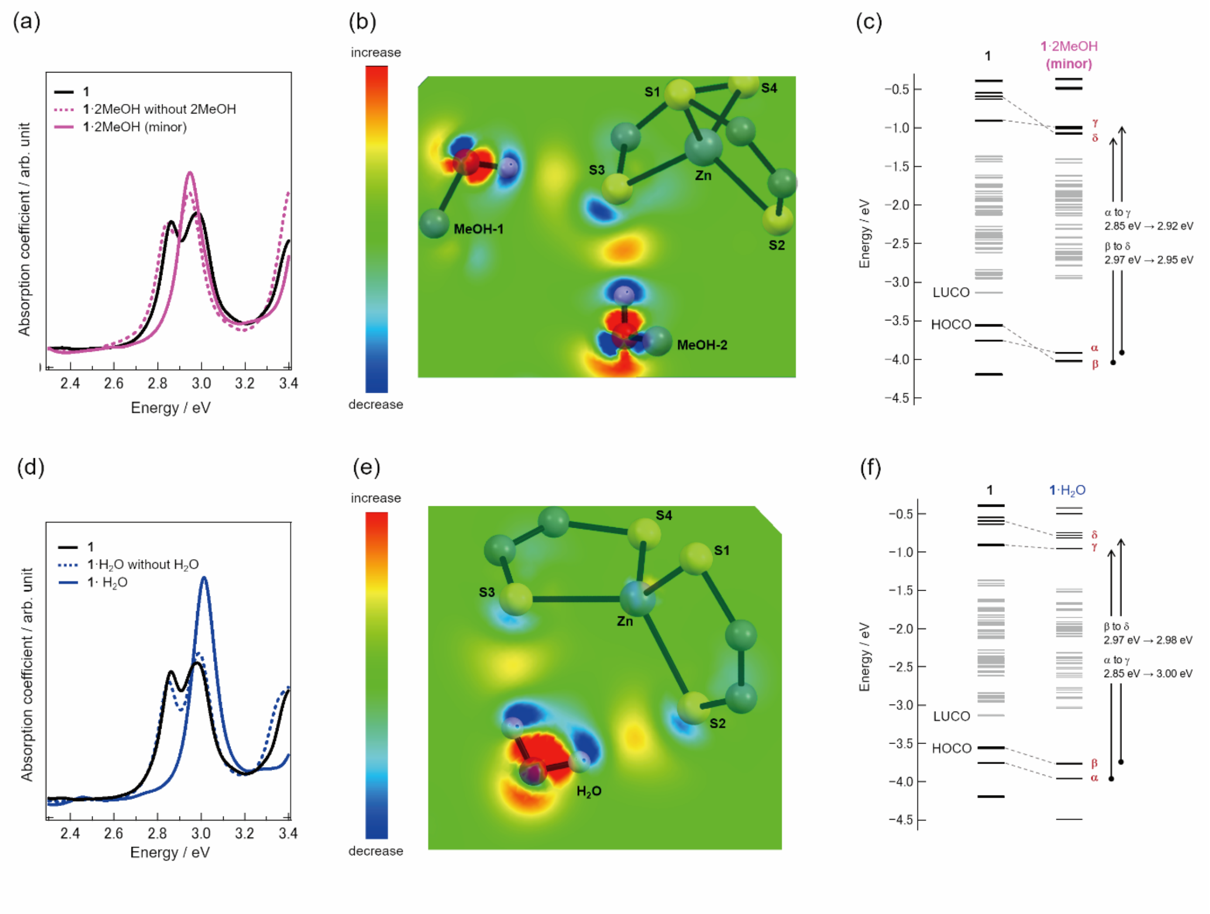

Fig. S10. (a)–(c): (a) The calculated absorption spectra, (b) the differential electron density map, and (c) crystal orbital energies of **1**·2MeOH (minor). (d)–(f): (d) The calculated absorption spectra, (e) the differential electron density map, and (f) crystal orbital energies of **1**·H_2O. The Red/blue region shows an increase/decrease of electron density by H-bonding formation.

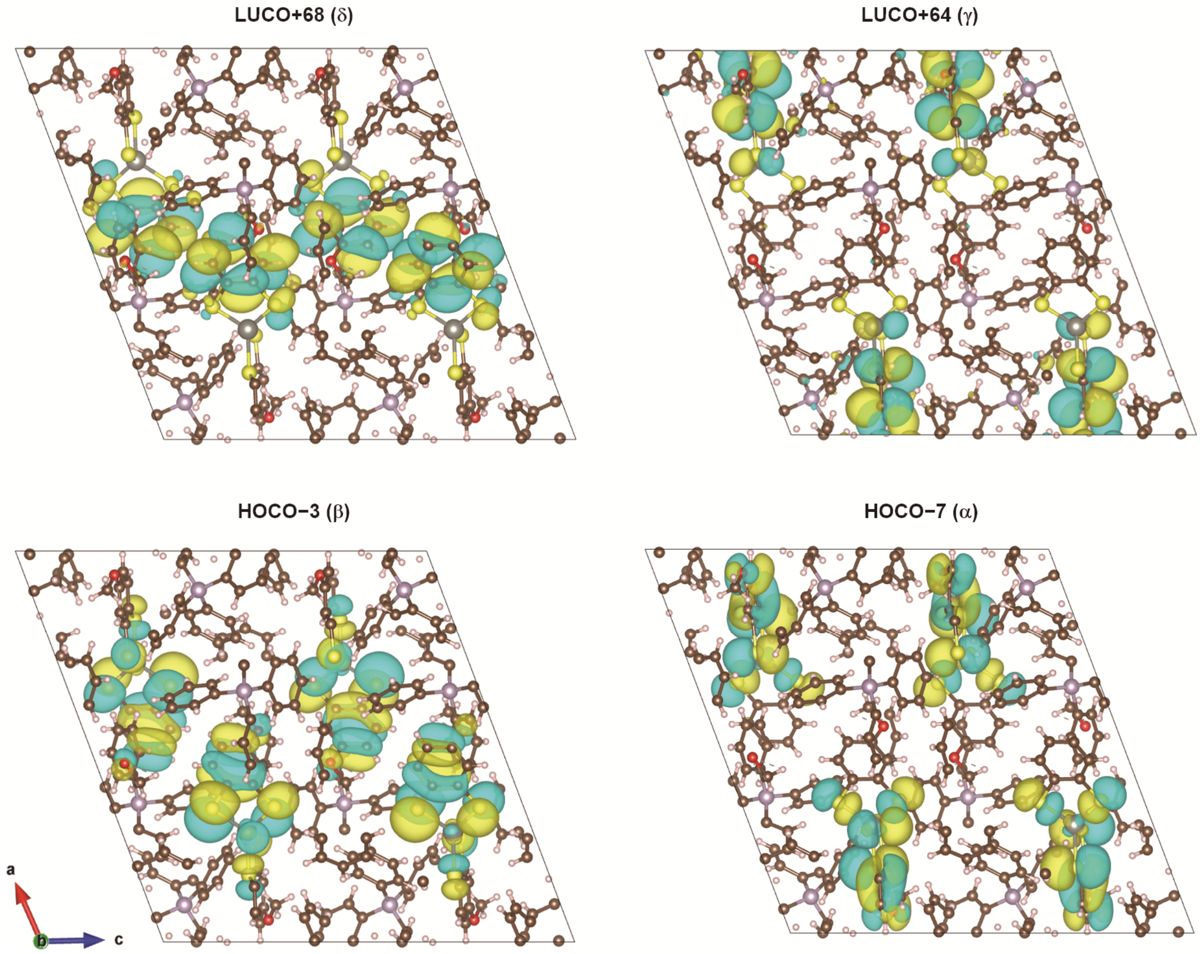

Fig. S11. Distributions of HOCO−7, HOCO−3, LUCO+64, and LUCO+68 in **1** (α: HOCO−7 to HOCO−4, β: HOCO−3 to HOCO, γ: LUCO+64 to LUCO+67, δ: LUCO+68 to LUCO+71).

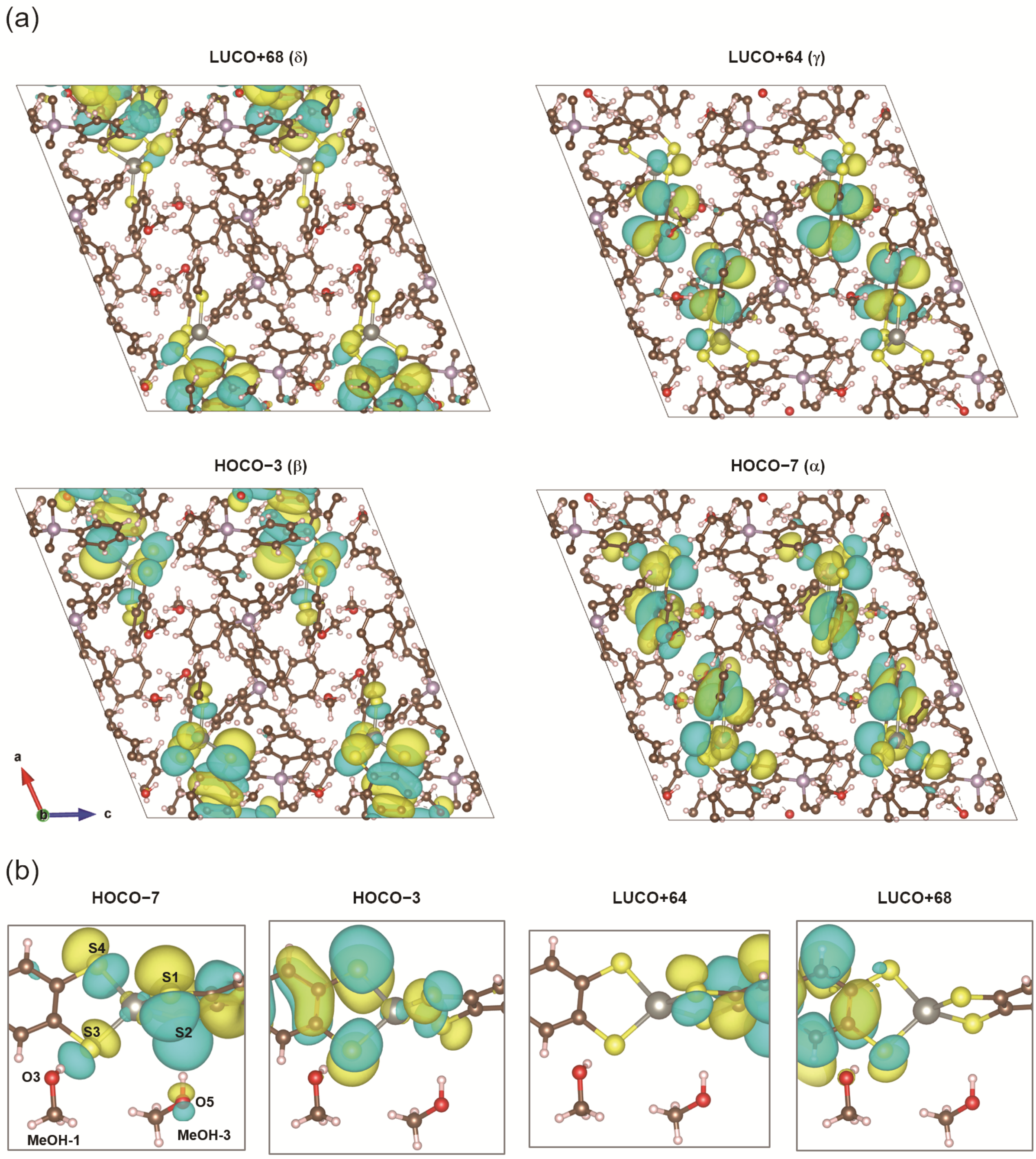

Fig. S12. (a) Distributions of HOCO−7, HOCO−3, LUCO+64, and LUCO+68 in **1**·2MeOH (major) (α: HOCO−7 to HOCO−4, β: HOCO−3 to HOCO, γ: LUCO+64 to LUCO+67, δ: LUCO+68 to LUCO+71). (b) Interactions between molecular orbitals of $[\mathrm{Zn(4\text{-}mxbdt)_2}]^{2-}$ complex and methanol molecule in the H-bonding part.

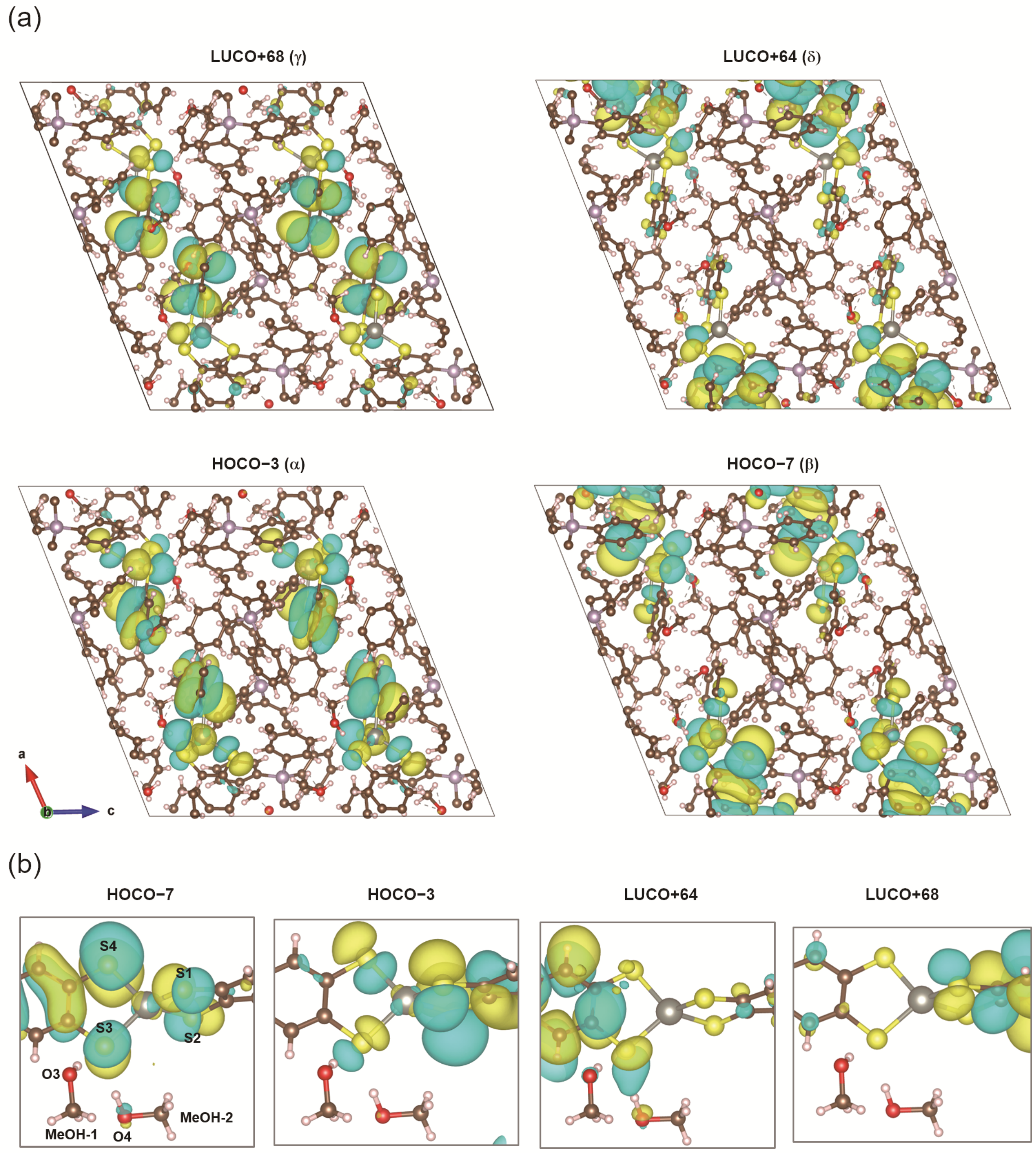

Fig. S13. (a) Distributions of HOCO−7, HOCO−3, LUCO+64, and LUCO+68 in **1**·2MeOH (minor) (β: HOCO−7 to HOCO−4, α: HOCO−3 to HOCO, δ: LUCO+64 to LUCO+67, γ: LUCO+68 to LUCO+71). (b) Interactions between molecular orbitals of $[\mathrm{Zn(4\text{-}mxbdt)_2}]^{2-}$ complex and methanol molecule in the H-bonding part.

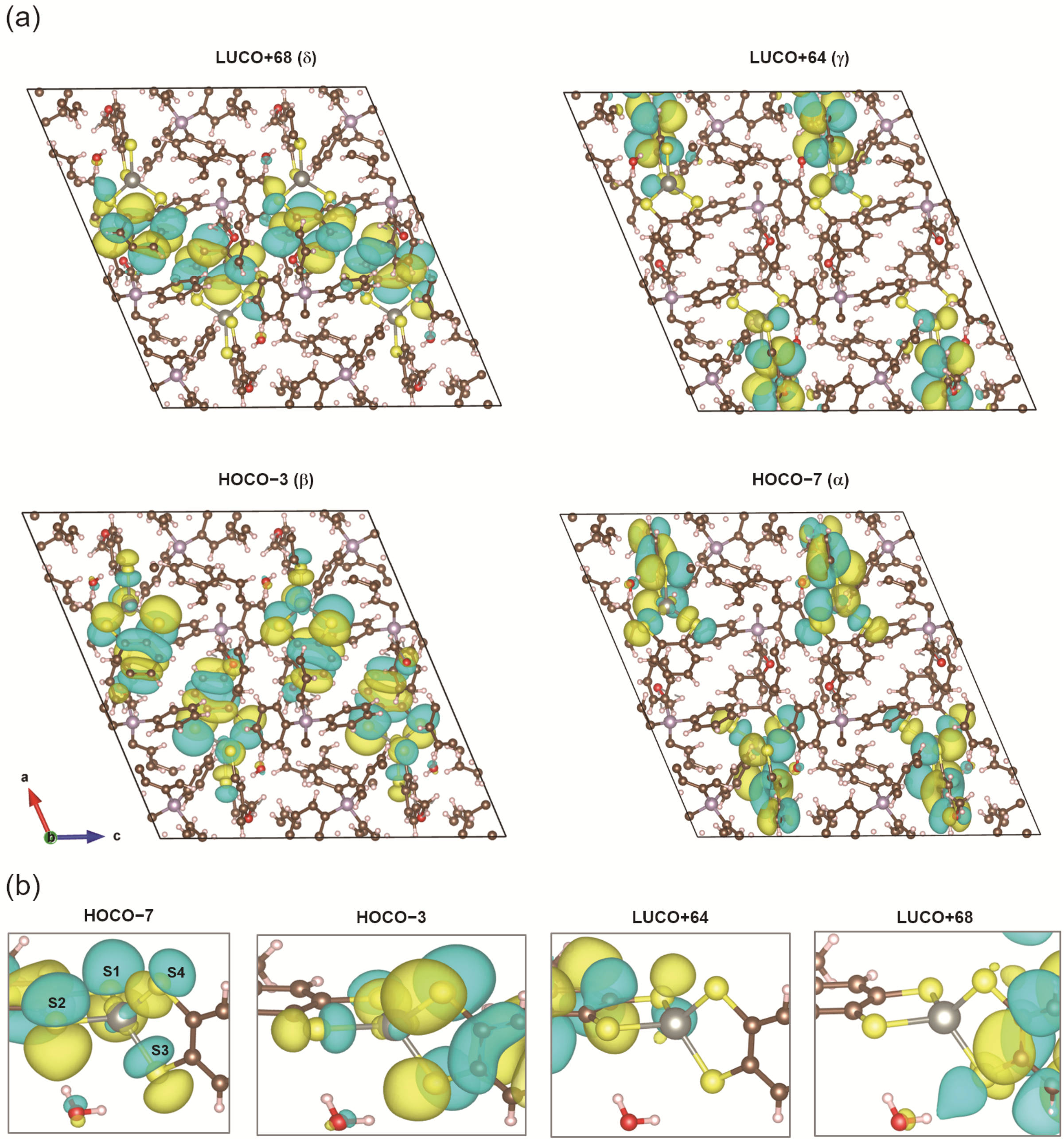

Fig. S14. (a) Distributions of HOCO−7, HOCO−3, LUCO+64, and LUCO+68 in **1**·H_2O (α: HOCO−7 to HOCO−4, β: HOCO−3 to HOCO, γ: LUCO+64 to LUCO+67, δ: LUCO+68 to LUCO+71). (b) Interaction between molecular orbitals of $[Zn(4\text{-}mxbdt)_2]^{2-}$ complex and water molecule in the H-bonding part.

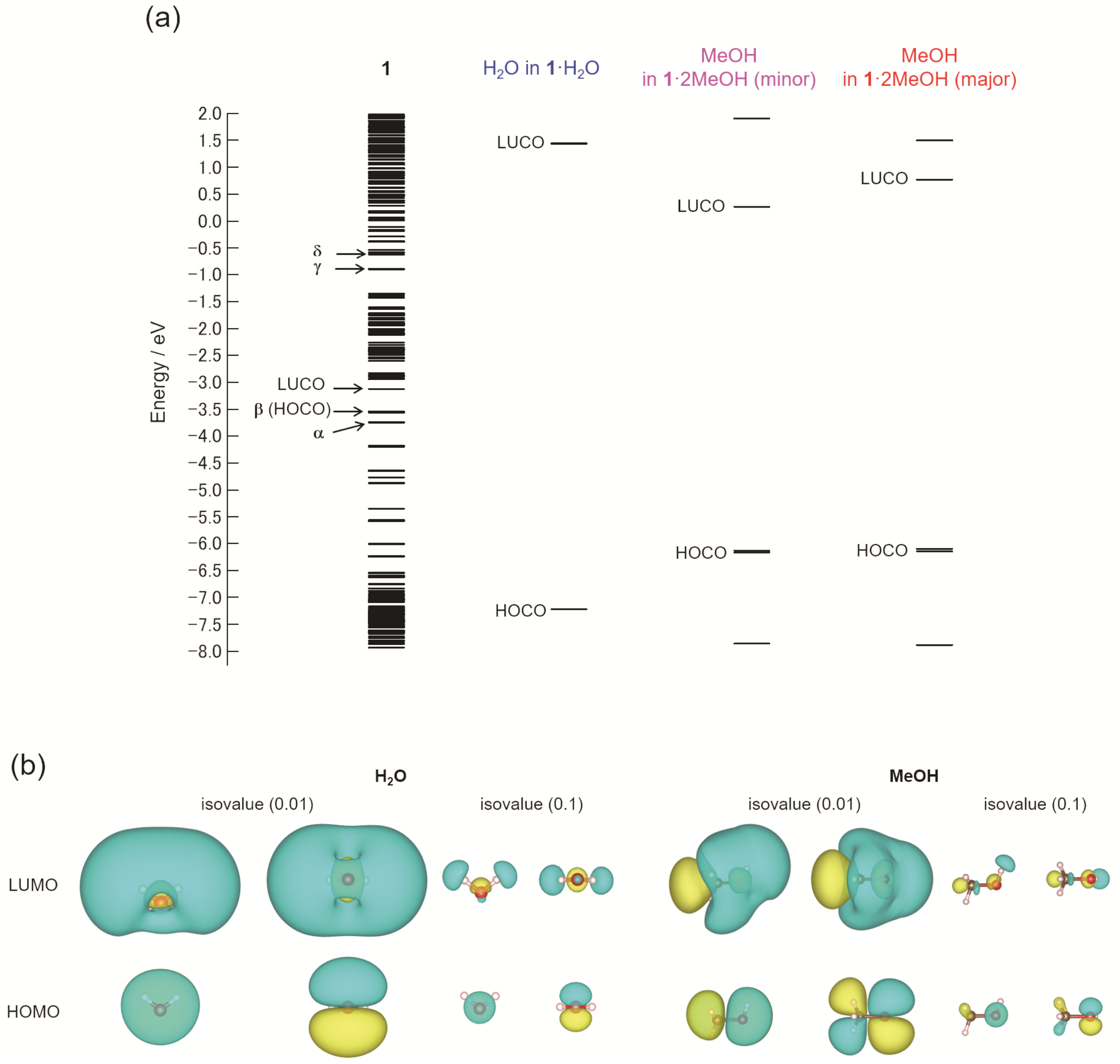

Fig. S15. (a) Energies of the frontier orbitals of the [Zn(4-mxbdt)$_2$]$^{2-}$ complexes and the vapor molecules in each crystal. (b) Distributions of the frontier orbitals of the vapor molecules (methanol: MeOH-1 in **1**·2MeOH, water: H_2O in **1**·H_2O).

The phase of the wave function in the H-bonding part was the same, and the shape of the crystal orbital on the S atom was deformed toward the H atom (Fig. S12b, S13b, and S14b). These show that the orbitals of the absorbed vapor molecule and the [Zn(4-mxbdt)$_2$]$^{2-}$ complex were hybridized to form bonding orbitals. Here, focusing on the distribution of HOMO and LUMO of the isolated water and methanol molecules (Fig. S15b), the HOMO forms π-bonding like interaction, whereas LUMO forms σ-bonding like interaction with surrounding orbitals. Because the shapes around [S···H–O]-type H-bonds were σ-type bonds in the crystals (Fig. S12b, S13b, and S14b), α, β, γ, and δ correspond to the bonding orbitals between HOMO (α and β) or LUMO (γ and δ) of the $[Zn(4\text{-}mxbdt)_2]^{2-}$ complex and LUMO of the absorbed vapor molecules, where the hybridization stabilizes the orbital energies of the $[Zn(4\text{-}mxbdt)_2]^{2-}$ complex. This hybridization also causes electron transfer from $[Zn(4\text{-}mxbdt)_2]^{2-}$ complex to the absorbed vapor molecules, which is consistent with the electron transfer indicated by Mulliken population analyses and the calculated differential electron density maps.

Next, we consider the difference in the degree of stabilization between the α/β and the γ/δ orbital groups. As shown in Fig. 4c left and S10, the energies of α/β and γ/δ were stabilized by the orbital hybridization with the electron transfer. However, the degree of stabilization of α/β was larger than that of γ/δ. As mentioned in the main text, this is because the α/β were largely distributed on the S atoms (S2 and S3) in the H-bonds than in the γ/δ. As a result, a stronger hybridization between the LUMO of the vapor molecules and the HOMO/LUMO of the $[Zn(4\text{-}mxbdt)_2]^{2-}$ complex and the decrease of charge density on the S atoms, as well as the electrostatic potential of $O^{\delta-}$–$H^{\delta+}$ part of the vapor molecules stabilize α/β more than γ/δ orbitals. These effects caused the blue shift in visible-light absorption observed in these crystals.

Comparing the distributions of HOCO−7 to HOCO and LUCO+64 to LUCO+71 in **1**·2MeOH (minor) and those in **1**·2MeOH (major) (Fig. S12 and S13), the energies of α and γ were exchanged with that of β and δ in **1**·2MeOH (minor), respectively. Here, the shape of α, β, γ and δ of **1**·2MeOH (major) and **1**·2MeOH (minor) is almost the same with those of **1**. As shown in Fig. S13b, the β and δ of **1**·2MeOH (minor) were largely distributed on the H-bonded S atom (S3). Therefore, because of doubly formed H-bonds with two methanol molecules to the S3 atom, the β and δ were more stabilized than the α and γ, resulting in the exchange of energy levels of the α, β, γ, and δ (Fig. S10c). This further supports the mechanism discussed above; the crystal orbitals largely distributed on the S atom (S3) forming H-bonds with methanol molecules were more stabilized with electron transfer (Fig. S10c and f). Note that the energy gap of the β to δ increased from 2.85 to 2.92 eV whereas that of the α to γ decreased from 2.97 to 2.95 eV due to this stabilization. However, consequently, the lowest energy transition in the visible-light region increased from 2.85 to 2.92 eV to lead the blue shift of visible-light absorption. Therefore, we concluded that the crystal orbital energies in **1**·2MeOH (major) were modulated by the same mechanism in **1**·2MeOH (major)

Table S9. Energies of crystal orbitals of α (HOCO−7 to HOCO−4), β (HOCO−3 to HOCO), γ (LUCO+64 to LUCO+67), and δ (LUCO+68 to LUCO+71) in each crystal.

Crystals	**1**	**1**·H_2O	**1**·2MeOH (minor)	**1**·2MeOH (major)
Crystal orbitals	Energy (eV)	Energy (eV)	Energy (eV)	Energy (eV)
HOCO−7	−3.76345937	−3.96134027	−4.02732	−4.09177
HOCO−6	−3.75930629	−3.9590735	−4.02374	−4.08713
HOCO−5	−3.75666102	−3.95557378	−4.0136	−4.08271
HOCO−4	−3.75586814	−3.95506278	−4.0135	−4.08233
Average (α)	−3.7588237	−3.95776258	−4.01954	−4.08598
HOCO−3	−3.57027136	−3.76997006	−3.92155	−3.93133
HOCO−2	−3.56592376	−3.76777623	−3.9197	−3.92969
HOCO−1	−3.55466646	−3.7583355	−3.91729	−3.92087
HOCO	−3.5523635	−3.75665251	−3.91653	−3.92019
Average (β)	−3.56080627	−3.76318358	−3.91877	−3.92552
LUCO+64	−0.91431822	−0.95650044	−1.08336	−1.07434
LUCO+65	−0.91118945	−0.95491357	−1.07044	−1.06703
LUCO+66	−0.90750922	−0.95330274	−1.07027	−1.06262
LUCO+67	−0.90178345	−0.95053919	−1.06986	−1.05126
Average (γ)	−0.90870008	−0.95381398	−1.07348	−1.06381
LUCO+68	−0.63176918	−0.81003675	−1.00706	−0.94296
LUCO+69	−0.59571851	−0.78422894	−0.99679	−0.93528
LUCO+70	−0.5917281	−0.78017894	−0.99407	−0.93391
LUCO+71	−0.54730391	−0.74831665	−0.98378	−0.92928
Average (δ)	−0.59162993	−0.78069032	−0.99542	−0.93536

Supplementary movie

Supplementary Movie S1: vapochromism in both visible-light absorption and photoluminescence from **1** to **1**·H_2O under the atmosphere (excitation wavelength: 365 nm). This movie was recorded at room temperature under the atmosphere (RH = 57%). The yellow powder is polycrystals of **1**·H_2O, and the orange powder is polycrystals of **1** prepared under N_2. Digital Temperature and Humidity Monitor: THA–01M (AS ONE Corporation). Handheld UV lamp: UVGL–58 (Analytik Jena US, An Endress+Hauser Company).

References

1 R. S. Mulliken, *J. Chem. Phys.,* 1955, **23**, 1833–1840.